

# Neutron skin of $^{48}\text{Ca}$ deduced from reaction and interaction cross sections

Shingo Tagami,<sup>1</sup> Masayuki Matsuzaki,<sup>2</sup> Jun Matsui,<sup>1</sup> and Masanobu Yahiro<sup>1,\*</sup>

<sup>1</sup>Department of Physics, Kyushu University, Fukuoka 819-0395, Japan

<sup>2</sup>Department of Physics, Fukuoka University of Education, Munakata, Fukuoka 811-4192, Japan

**Background:** In our previous paper, we predicted reaction cross sections  $\sigma_R$  for  $^{40-60,62,64}\text{Ca} + ^{12}\text{C}$  scattering at 280 MeV per nucleon, using the Kyushu (chiral)  $g$ -matrix folding model with the densities calculated with the Gogny-D1S Hartree-Fock-Bogoliubov (D1S-GHFB) with and without the angular momentum projection (AMP). Interaction cross sections  $\sigma_I (\approx \sigma_R)$  are available for  $^{42-51}\text{Ca} + ^{12}\text{C}$  scattering, whereas  $\sigma_R$  are available for  $p + ^{48}\text{Ca}$  scattering. As for  $^{48}\text{Ca}$ , the high-resolution  $E1$  polarizability experiment ( $E1pE$ ) yields  $r_{\text{skin}}^{48}(E1pE) = 0.14 \sim 0.20$  fm.

**Purpose:** We determine  $r_{\text{skin}}^{48}(\text{exp})$  from the data on  $\sigma_R$  for  $p + ^{48}\text{Ca}$  scattering and from the data on  $\sigma_I$  for  $^{48}\text{Ca} + ^{12}\text{C}$  scattering.

**Methods:** We use the chiral (Kyushu)  $g$ -matrix folding model with the densities calculated with the Gogny-D1M Hartree-Fock-Bogoliubov with the AMP, i. e., D1M-GHFB+AMP. The D1M-GHFB+AMP proton and neutron densities are scaled so as to reproduce the data under the condition that the radius  $r_p$  of the scaled proton density equals the data  $r_p(\text{exp})$  determined from the electron scattering. The neutron radius  $r_n$  thus obtained is an experimental value.

**Results:** Our results are  $r_{\text{skin}}^{48}(\text{exp}) = -0.031 \sim 0.183$  fm for  $p + ^{48}\text{Ca}$  scattering and  $0.100 \sim 0.218$  fm for  $^{48}\text{Ca} + ^{12}\text{C}$  scattering. Using the  $r_{\text{skin}}^{48} - r_{\text{skin}}^{208}$  relation with a high correlation coefficient  $R = 0.99$ , we have transformed  $r_{\text{skin}}^{208}(\text{PREXII})$  and  $r_{\text{skin}}^{208}(E1pE)$  to the corresponding values  $r_{\text{skin}}^{48}(\text{tPREXII})$  and  $r_{\text{skin}}^{48}(\text{t}E1pE)$ , where the symbol ‘t’ stands for the transformed data. The transformed data  $r_{\text{skin}}^{48}(\text{tPREXII}) = 0.190 \sim 0.268$  fm is consistent with  $r_{\text{skin}}^{48} = 0.102 \sim 0.218$  fm for  $^{48}\text{Ca} + ^{12}\text{C}$  scattering.

**Conclusion:** Our final result is  $r_{\text{skin}}^{48} = 0.102 \sim 0.218$  fm determined from  $^{48}\text{Ca} + ^{12}\text{C}$  scattering.

## I. INTRODUCTION AND CONCLUSION

*Background on experiments.* Neutron skin thickness  $r_{\text{skin}}$  is strongly correlated with the slope parameter in the symmetric energy of nuclear matter [1, 2]. The  $r_{\text{skin}}$  is thus important to determine the EoS.

Horowitz, Pollock and Souder proposed a direct measurement for  $r_{\text{skin}} = r_n - r_p$  [3], where  $r_p$  and  $r_n$  are proton and neutron radii, respectively. The measurement consists of parity-violating and elastic electron scattering. In fact, the PREX collaboration has reported a new value,

$$r_{\text{skin}}^{208}(\text{PREXII}) = 0.283 \pm 0.071 \text{ fm}, \quad (1)$$

combining the original Lead Radius EXperiment (PREX) result [4, 5] with the updated PREX-II result [6]. The value is most reliable for  $r_{\text{skin}}^{208}$ . For  $^{48}\text{Ca}$ , the CREX is still ongoing at Jefferson Lab [7].

As an indirect measurement on  $r_{\text{skin}}$ , the high-resolution  $E1$  polarizability experiment ( $E1pE$ ) was made for  $^{208}\text{Pb}$  [8] and  $^{48}\text{Ca}$  [9] in RCNP. The results are

$$r_{\text{skin}}^{208}(E1pE) = 0.156_{-0.021}^{+0.025} = 0.135 \sim 0.181 \text{ fm}, \quad (2)$$

$$r_{\text{skin}}^{48}(E1pE) = 0.14 \sim 0.20 \text{ fm}. \quad (3)$$

For  $^{208}\text{Pb}$ , the central value 0.156 fm of the indirect measurement is much smaller than 0.283 fm of the direct measurement. This is a problem to be solved.

Reaction cross section  $\sigma_R$  is a standard observable to determine the matter radius  $r_m$ . The  $\sigma_R(\text{exp})$  are available for  $p + ^{48}\text{Ca}$  scattering in incident energies of  $E_{\text{in}} = 23 \sim 48$  MeV [10].

Very lately, Tanaka *et al.* published data on interaction cross sections  $\sigma_I (\approx \sigma_R)$  for  $^{42-51}\text{Ca} + ^{12}\text{C}$  scattering at 280 MeV per nucleon [11]. The data for  $^{42-51}\text{Ca} + ^{12}\text{C}$  have higher accuracy than the data for  $p + ^{48}\text{Ca}$ , since the former has 1% errors but the latter has 4% errors. They determined matter radii  $r_m(\sigma_I)$  from the  $\sigma_I$  using the optical limit of the Glauber model with the Wood-Saxon density, and deduced  $r_{\text{skin}}(\sigma_I)$  and  $r_n(\sigma_I)$  from the  $r_m(\sigma_I)$  and the  $r_p(\text{exp})$  [12] deduced from the electron scattering. Tanaka *et al.* provide us the numerical values of  $r_m(\sigma_I)$ ,  $r_{\text{skin}}(\sigma_I)$ ,  $r_n(\sigma_I)$ . As for  $r_{\text{skin}}^{48}$ , their result is

$$r_{\text{skin}}^{48}(\sigma_I) = 0.086 \sim 0.206 \text{ fm}. \quad (4)$$

*Background on theories:* As an *ab initio* method for Ca isotopes, we should consider the coupled-cluster method [13, 14] with chiral interaction. The coupled-cluster result [14]

$$r_{\text{skin}}^{48}(\text{CC}) = 0.12 \sim 0.15 \text{ fm} \quad (5)$$

is consistent with data  $r_{\text{skin}}^{48}(E1pE)$  and  $r_{\text{skin}}^{48}(\sigma_I)$ .

Kohno calculated the  $g$  matrix for the symmetric nuclear matter, using the Brueckner-Hartree-Fock method with chiral  $N^3\text{LO}$  2NFs and NNLO 3NFs [15]. He set  $c_D = -2.5$  and  $c_E = 0.25$  so that the energy per nucleon can become minimum at  $\rho = \rho_0$ . Toyokawa *et al.* localized the non-local chiral  $g$  matrix into three-range Gaussian forms [16], using the localization method proposed by the Melbourne group [17, 18]. The resulting local  $g$  matrix is referred to as “Kyushu  $g$ -matrix”. The Kyushu  $g$ -matrix [16] is constructed from the chiral nucleon-nucleon (NN) interaction with the cut-off 550 MeV.

In our previous paper of Ref. [19], we tested the Kyushu  $g$ -matrix folding model [16, 20, 21] for  $^{12}\text{C} + ^{12}\text{C}$  scattering by comparing measured reaction cross section  $\sigma_R$  [22] with the theoretical results, and found that the model is reliable in

\* orion093g@gmail.com

$30 \lesssim E_{\text{in}} \lesssim 100$  MeV and  $250 \lesssim E_{\text{in}} \lesssim 400$  MeV. We then predicted reaction cross section  $\sigma_R$  for  $^{42-51}\text{Ca}$ . The prediction is shown in Fig. 1. For  $^{48}\text{Ca}$ , the result of the folding model with the D1S-GHFB+AMP densities agrees with the upper limit of  $\sigma_I (\approx \sigma_R)$ , where “D1S-GHFB+AMP” stands for the Gogny-D1S Hartree-Fock-Bogoliubov with the angular momentum projection (AMP). Our method is much better than the optical limit of the Glauber model with the Wood-Saxon density.

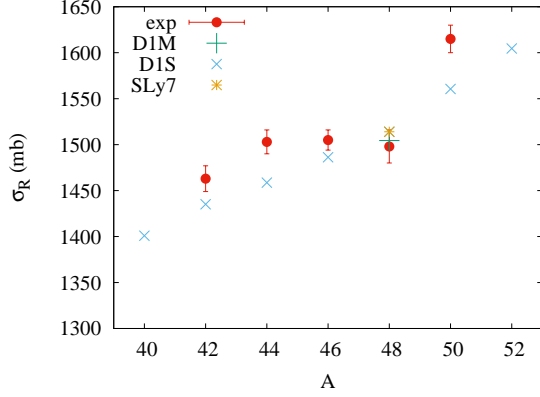


FIG. 1. Mass-number  $A$  dependence of  $\sigma_R$  for  $^{40-52}\text{Ca}+^{12}\text{C}$  scattering at 280 MeV per nucleon. The data are taken from Ref. [11] and the results of Kyushu  $g$ -matrix folding model with the D1S-GHFB+AMP densities are from Ref. [19]. For  $^{48}\text{Ca}$ , results of D1M-GHFB+AMP and SLy7-HFB are newly added. The difference between D1S-GHFB+AMP and SLy7-HFB is negligible, as shown in Sec. II.

*Purpose:* We determine experimental values of  $r_{\text{skin}}^{48}$  from the data on  $\sigma_R$  for  $p+^{48}\text{Ca}$  scattering in  $E_{\text{in}} = 30 \sim 48$  MeV and the data on  $\sigma_I$  for  $^{48}\text{Ca}+^{12}\text{C}$  scattering at  $E_{\text{in}} = 280$  MeV per nucleon scattering.

*Methods:* We use the Kyushu  $g$ -matrix folding model with the densities calculated with D1M-GHFB+AMP, and scale the D1M-GHFB+AMP proton and neutron densities so as to reproduce the data on  $\sigma_R$  for  $p+^{48}\text{Ca}$  scattering and  $\sigma_I (\approx \sigma_R)$  for  $^{48}\text{Ca}+^{12}\text{C}$  scattering under the condition that the radius  $r_p$  of the scaled proton density equals the data  $r_p(\text{exp})$  determined from the electron scattering. The neutron radius  $r_n$  thus obtained is an experimental value. Note that our method is much better than the optical limit of the Glauber model with the Wood-Saxon density.

*Conclusion:* Our final result is

$$r_{\text{skin}}^{48}(\text{exp}) = 0.160 \pm 0.058 \text{ fm} = 0.102 \sim 0.218 \text{ fm} \quad (6)$$

deduced from  $^{48}\text{Ca}+^{12}\text{C}$  scattering at  $E_{\text{in}} = 280$  MeV per nucleon scattering, since the data for  $^{42-51}\text{Ca} + ^{12}\text{C}$  have higher accuracy than the data for  $p+^{48}\text{Ca}$ .

## II. KYUSHU $g$ -MATRIX FOLDING MODEL

The Kyushu  $g$ -matrix folding model is successful in reproducing  $\sigma_R$  and differential cross sections  $d\sigma/d\Omega$  for  $^4\text{He}$  scattering in  $E_{\text{in}} = 30 \sim 200$  MeV per nucleon [16]. This is the case for  $^{12}\text{C}$  scattering on  $^9\text{Be}$ ,  $^{12}\text{C}$ ,  $^{27}\text{Al}$  targets in  $30 \lesssim E_{\text{in}} \lesssim 100$  MeV and  $250 \lesssim E_{\text{in}} \lesssim 400$  MeV [19]. The success is true for proton scattering at  $E_{\text{in}} = 65$  MeV [20].

In this paper, therefore, we use the Kyushu  $g$ -matrix folding model not only for  $p+^{48}\text{Ca}$  scattering in  $E_{\text{in}} = 30 \sim 48$  MeV where our model is reliable but also for  $^{48}\text{Ca}+^{12}\text{C}$  scattering at  $E_{\text{in}} = 280$  MeV per nucleon where our model is reliable. As the proton and neutron densities,  $\rho_p(r)$  and  $\rho_n(r)$  for  $^{48}\text{Ca}$ , we use D1M-GHFB+AMP, D1S-GHFB+AMP, SLy7-HFB. As a way of taking the center-of-mass correction to the densities, we use the method of Ref. [23], since the procedure is quite simple.

As show in Fig. 2, we find that the densities of D1S-GHFB+AMP are almost the same as those of SLy7-HFB where SLy7 [24–26] is an improved version of SLy4 [24–26]. The SLy7-HFB is quite useful, since the densities of SLy7 is almost the same as those of D1S-GHFB+AMP.

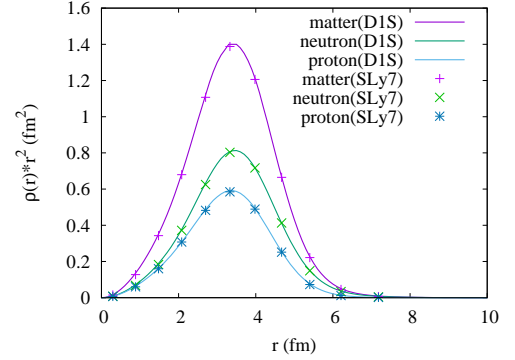


FIG. 2. Second moments of matter, neutron, and proton densities of D1S-GHFB+AMP and SLy7-HFB.

### 1. Single folding model for $p+^{48}\text{Ca}$ scattering

The potential  $U(\mathbf{R})$  is composed of the direct and exchange parts,  $U^{\text{DR}}(\mathbf{R})$  and  $U^{\text{EX}}(\mathbf{R})$  [27, 28]: Namely,

$$U(\mathbf{R}) = U^{\text{DR}}(\mathbf{R}) + U^{\text{EX}}(\mathbf{R}) \quad (7)$$

with

$$U^{\text{DR}}(\mathbf{R}) = \sum_{\nu} \int \rho_{\text{T}}^{\nu}(\mathbf{r}_{\text{T}}) g_{\mu\nu}^{\text{DR}}(s; \rho_{\mu\nu}) d\mathbf{r}_{\text{T}}, \quad (8)$$

$$U^{\text{EX}}(\mathbf{R}) = \sum_{\nu} \int \rho_{\text{T}}^{\nu}(\mathbf{r}_{\text{T}}, \mathbf{r}_{\text{T}} + \mathbf{s}) \times g_{\mu\nu}^{\text{EX}}(s; \rho_{\mu\nu}) \exp[-i\mathbf{K}(\mathbf{R}) \cdot \mathbf{s}/M] d\mathbf{r}_{\text{T}}, \quad (9)$$

where  $\mu = -1/2$ , the coordinate  $\mathbf{R}$  stands for the relative coordinate between an incident nucleon and a target (T), and

$\mathbf{s} \equiv -\mathbf{r}_T + \mathbf{R}$  for the coordinate  $\mathbf{r}_T$  of the interacting nucleon from T. Each of  $\mu$  and  $\nu$  denotes the  $z$ -component of isospin;  $1/2$  means neutron and  $-1/2$  does proton. The nonlocal  $U^{\text{EX}}$  has been localized in Eq. (9) with the local semi-classical approximation [29–31], where  $\mathbf{K}(\mathbf{R})$  is the local momentum between the incident proton and T, and  $M = A_T/(1 + A_T)$  for the target mass number  $A_T$ . The validity of this localization is shown in Ref. [27].

The direct and exchange parts,  $g_{\mu\nu}^{\text{DR}}$  and  $g_{\mu\nu}^{\text{EX}}$ , of the  $g$ -matrix depend on the local density

$$\rho_{\mu\nu} = \rho_T^\nu(\mathbf{r}_T + \mathbf{s}/2) \quad (10)$$

at the midpoint of the interacting nucleon pair, where  $\mu = -1/2$ .

The direct and exchange parts,  $g_{\mu\nu}^{\text{DR}}$  and  $g_{\mu\nu}^{\text{EX}}$ , of the  $g$ -matrix are described by

$$\begin{aligned} & g_{\mu\nu}^{\text{DR}}(s; \rho_{\mu\nu}) \\ &= \begin{cases} \frac{1}{4} \sum_S \hat{S}^2 g_{\mu\nu}^{S1}(s; \rho_{\mu\nu}) & ; \text{ for } \mu + \nu = \pm 1 \\ \frac{1}{8} \sum_{S,T} \hat{S}^2 g_{\mu\nu}^{ST}(s; \rho_{\mu\nu}), & ; \text{ for } \mu + \nu = 0 \end{cases} \quad (11) \\ & g_{\mu\nu}^{\text{EX}}(s; \rho_{\mu\nu}) \\ &= \begin{cases} \frac{1}{4} \sum_S (-1)^{S+1} \hat{S}^2 g_{\mu\nu}^{S1}(s; \rho_{\mu\nu}) & ; \text{ for } \mu + \nu = \pm 1 \\ \frac{1}{8} \sum_{S,T} (-1)^{S+T} \hat{S}^2 g_{\mu\nu}^{ST}(s; \rho_{\mu\nu}) & ; \text{ for } \mu + \nu = 0 \end{cases} \quad (12) \end{aligned}$$

where  $\hat{S} = \sqrt{2S+1}$  and  $g_{\mu\nu}^{ST}$  are the spin-isospin components of the  $g$ -matrix.

The  $\sigma_R$  is sensitive to the root-mean-square matter point-radius,  $\sqrt{\langle \mathbf{r}^2 \rangle_T}$ , of T; namely,

$$\sigma_R = C\pi \left[ \sqrt{\langle \mathbf{r}^2 \rangle_T} \right]^2 \quad (13)$$

for a constant  $C$ .

## 2. Double folding model for $^{48}\text{Ca} + ^{12}\text{C}$ scattering

For nucleus-nucleus (P+T) scattering, the potential  $U(\mathbf{R})$  is  $U^{\text{DR}} + U^{\text{EX}}$  defined by

$$\begin{aligned} U^{\text{DR}}(\mathbf{R}) &= \sum_{\mu,\nu} \int \rho_P^\mu(\mathbf{r}_P) \rho_T^\nu(\mathbf{r}_T) g_{\mu\nu}^{\text{DR}}(s; \rho_{\mu\nu}) d\mathbf{r}_P d\mathbf{r}_T, \quad (14) \\ U^{\text{EX}}(\mathbf{R}) &= \sum_{\mu,\nu} \int \rho_P^\mu(\mathbf{r}_P, \mathbf{r}_P - \mathbf{s}) \rho_T^\nu(\mathbf{r}_T, \mathbf{r}_T + \mathbf{s}) \\ &\quad \times g_{\mu\nu}^{\text{EX}}(s; \rho_{\mu\nu}) \exp[-i\mathbf{K}(\mathbf{R}) \cdot \mathbf{s}/M_A] d\mathbf{r}_P d\mathbf{r}_T(15) \end{aligned}$$

where  $\mathbf{s} = \mathbf{r}_P - \mathbf{r}_T + \mathbf{R}$  for the coordinate  $\mathbf{R}$  between P and T. The coordinate  $\mathbf{r}_P$  ( $\mathbf{r}_T$ ) denotes the location of an interacting nucleon measured from the center-of-mass of the projectile (target). The original form of  $U^{\text{EX}}$  is a non-local function of  $\mathbf{R}$ , but it has been localized in Eq. (15) with the local

semi-classical approximation [29–31] where P is assumed to propagate as a plane wave with the local momentum  $\hbar\mathbf{K}(\mathbf{R})$  within a short range of the nucleon-nucleon interaction, where  $M_A = AA_T/(A + A_T)$  for the mass number  $A$  ( $A_T$ ) of P (T).

The direct and exchange parts,  $g_{\mu\nu}^{\text{DR}}$  and  $g_{\mu\nu}^{\text{EX}}$ , of the effective nucleon-nucleon interaction ( $g$ -matrix) are assumed to depend on the local density

$$\rho_{\mu\nu} = \rho_P^\mu(\mathbf{r}_P - \mathbf{s}/2) + \rho_T^\nu(\mathbf{r}_T + \mathbf{s}/2) \quad (16)$$

at the midpoint of the interacting nucleon pair. As for  $^{12}\text{C}$ , we use a phenomenological density of Ref. [32].

The  $\sigma_R$  is sensitive to the root-mean-square matter radii,  $\sqrt{\langle \mathbf{r}^2 \rangle_P}$  and  $\sqrt{\langle \mathbf{r}^2 \rangle_T}$ , of P and T, respectively [23]: Namely,

$$\sigma_R = C\pi \left[ \sqrt{\langle \mathbf{r}^2 \rangle_P} + \sqrt{\langle \mathbf{r}^2 \rangle_T} \right]^2 \quad (17)$$

for a constant  $C$ .

## III. RESULTS

A mentioned in Sec. I, the Kyushu  $g$ -matrix folding model [16, 20, 21] is reliable in  $30 \lesssim E_{\text{in}} \lesssim 100$  MeV and  $250 \lesssim E_{\text{in}} \lesssim 400$  MeV.

Particularly for  $^{48}\text{Ca} + ^{12}\text{C}$  scattering at  $E_{\text{in}} = 280$  MeV per nucleon, as shown in Fig 1, three theoretical results of D1M-DHFB+AMP, D1S-DHFB+AMP, SLy7-HFB reproduce the data [11] on  $\sigma_I$ . The difference between D1S-GHFB+AMP and SLy7-HFB is negligible, since the relative difference between D1S-GHFB+AMP and SLy7-HFB is 0.06%.

Now we use the D1M-GHFB+AMP proton and neutron and densities for  $^{48}\text{Ca}$ , since D1M [33, 34] is an improved version of D1S. We scale the densities so that the  $\sigma_R$  calculated from the scaled densities can agree with  $\sigma_I$  under the condition that the  $r_p$  of the scaled proton density equals  $r_p(\text{exp}) = 3.397$  fm [35] deduced by electron scattering.

The  $r_m(\text{exp})$  thus obtained is  $3.456 \sim 3.526$  fm. We obtain  $r_{\text{skin}}^{48}(\text{exp}) = 0.102 \sim 0.218$  fm and  $r_n(\text{exp}) = 3.497 \sim 3.615$  fm from the  $r_m(\text{exp})$  and the  $r_p(\text{exp})$ .

Figure 3 shows reaction cross sections  $\sigma_R$  for  $p + ^{48}\text{Ca}$  scattering in  $E_{\text{in}} = 23 \sim 48$  MeV. In  $E_{\text{in}} = 30 \sim 48$  MeV where the Kyushu  $g$ -matrix model is reliable, the results of D1M-DHFB+AMP are near the upper bound of the data [10], whereas the results of D1S-GHFB+AMP and SLy7-HFB somewhat overshoot the upper bound; note that the relative difference between D1S-GHFB+AMP and SLy7-HFB is 0.1%.

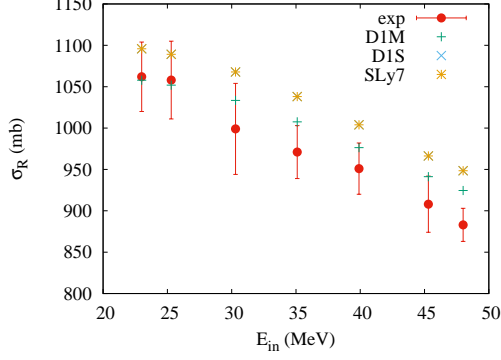


FIG. 3. Reaction cross sections for  $p+^{48}\text{Ca}$  scattering in  $E_{\text{in}} = 23 \sim 48$  MeV. Symbol “+” stands for the result of D1M-DHFB+AMP, whereas “ $\times$ ” (“\*”) corresponds to that of D1S-DHFB+AMP (SLy7-HFB). Note that the difference between D1S-DHFB+AMP and SLy7-HFB is negligible. The data are taken from Ref. [10].

We scale the proton and neutron densities of D1M-DHFB+AMP so that results of the scaled densities can reproduce measured  $\sigma_R$  for  $p+^{48}\text{Ca}$  scattering in  $E_{\text{in}} = 30 \sim 48$  MeV under the condition that the radius  $r_p$  of the scaled proton density agrees with  $r_p(\text{exp}) = 3.3971$  fm [35] of electron scattering. The  $r_m(\text{exp})$  thus obtained depend on  $E_{\text{in}}$ . We then take the weighted mean and its error for five  $E_{\text{in}}$  in  $E_{\text{in}} = 30 \sim 48$  MeV. The resulting  $r_m(\text{exp})$  is  $3.379 \sim 3.505$  fm. We obtain  $r_{\text{skin}}^{48}(\text{exp}) = -0.031 \sim 0.183$  fm and  $r_n(\text{exp}) = 3.366 \sim 3.580$  fm from the  $r_m(\text{exp})$  and the  $r_p(\text{exp})$ .

Eventually, we determine two values on  $r_{\text{skin}}^{48}(\text{exp})$ , i.e.,

$$r_{\text{skin}}^{48}(\text{exp}) = -0.031 \sim 0.183 \text{ fm} \quad (18)$$

for  $p+^{48}\text{Ca}$  scattering in  $E_{\text{in}} = 30 \sim 48$  MeV and

$$r_{\text{skin}}^{48}(\text{exp}) = 0.102 \sim 0.218 \text{ fm} \quad (19)$$

for  $^{48}\text{Ca} + ^{12}\text{C}$  scattering at 280 MeV per nucleon.

Using the  $r_{\text{skin}}^{48} - r_{\text{skin}}^{208}$  relation with a high correlation coefficient  $R = 0.99$  [36],

$$r_{\text{skin}}^{48} = 0.5547 r_{\text{skin}}^{208} + 0.0718, \quad (20)$$

we have transformed  $r_{\text{skin}}^{208}(\text{PREXII})$  and  $r_{\text{skin}}^{208}(E1pE)$  to the corresponding values  $r_{\text{skin}}^{48}(\text{tPREXII})$  and  $r_{\text{skin}}^{48}(tE1pE)$ , where the symbol ‘t’ stands for the transformed data. The transformed data are

$$r_{\text{skin}}^{48}(\text{tPREXII}) = 0.190 \sim 0.268 \text{ fm} \quad (21)$$

for PREX-II and

$$r_{\text{skin}}^{48}(tE1pE) = 0.147 \sim 0.172 \text{ fm} \quad (22)$$

for  $E1pE$ . The  $r_{\text{skin}}^{48}(tE1pE)$  is consistent with the original  $r_{\text{skin}}^{48}(E1pE)$ . This indicates that the transformation is reliable. Our results are compared with the data and the CC result, as shown in Fig. 4.

The  $r_{\text{skin}}^{48}(\text{exp}) = 0.102 \sim 0.218$  fm for  $^{48}\text{Ca} + ^{12}\text{C}$  scattering is better than the  $r_{\text{skin}}^{48}(\text{exp}) = -0.031 \sim 0.183$  fm for  $p+^{48}\text{Ca}$  scattering, when we consider  $r_{\text{skin}}^{48}(\text{tPREXII}) = 0.190 \sim 0.268$  fm as a reference data. In addition, the  $r_{\text{skin}}^{48}(\text{exp}) = -0.031 \sim 0.183$  fm has a larger error than the  $r_{\text{skin}}^{48}(\text{exp}) = 0.102 \sim 0.218$  fm.

Our final result is  $r_{\text{skin}}^{48}(\text{exp}) = 0.160 \pm 0.058$  fm =  $0.102 \sim 0.218$  fm deduced from  $^{48}\text{Ca} + ^{12}\text{C}$  scattering at 280 MeV per nucleon.

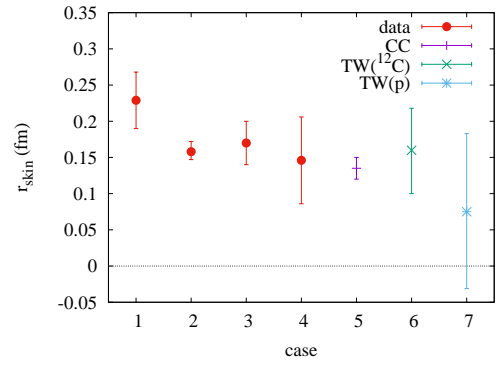


FIG. 4. Comparison among four data, the CC result and the result of this work; namely, cases “1 ~ 7” correspond to  $r_{\text{skin}}^{48}(\text{tPREX})$ ,  $r_{\text{skin}}^{48}(tE1pE)$ ,  $r_{\text{skin}}^{48}(E1pE)$ ,  $r_{\text{skin}}^{48}(\sigma_I)$ ,  $r_{\text{skin}}^{48}(\text{CC})$ ,  $r_{\text{skin}}^{48}(\text{TW, EXP, } ^{12}\text{C target})$ ,  $r_{\text{skin}}^{48}(\text{TW, EXP, p scattering})$ , respectively.

## ACKNOWLEDGEMENTS

We thank Dr. Tanaka and Prof. Fukuda for providing the data.

- [1] X. Roca-Maza, M. Centelles, X. Vinas, and M. Warda, Phys. Rev. Lett. **106**, 252501 (2011), arXiv:1103.1762 [nucl-th].
- [2] B. A. Brown, Phys. Rev. Lett. **111**, 232502 (2013), arXiv:1308.3664 [nucl-th].

- [3] C. J. Horowitz, S. J. Pollock, P. A. Souder, and R. Michaels, Phys. Rev. C **63**, 025501 (2001).
- [4] S. Abrahamyan, Z. Ahmed, H. Albatineh, K. Aniol, D. S. Armstrong, W. Armstrong, T. Averett, B. Babineau, A. Bar-

- bieri, V. Bellini, *et al.* (PREX Collaboration), *Phys. Rev. Lett.* **108**, 112502 (2012).
- [5] C. J. Horowitz, Z. Ahmed, C.-M. Jen, A. Rakhman, P. A. Souder, M. M. Dalton, N. Liyanage, K. D. Paschke, K. Saenboonruang, R. Silwal, G. B. Franklin, M. Friend, B. Quinn, K. S. Kumar, D. McNulty, L. Mercado, S. Riordan, J. Wexler, R. W. Michaels, and G. M. Urciuoli, *Phys. Rev. C* **85**, 032501 (2012).
- [6] D. Adhikari *et al.* (PREX), *Phys. Rev. Lett.* **126**, 172502 (2021), arXiv:2102.10767 [nucl-ex].
- [7] R. Michaels *et al.*, “Lead radius experiment prex proposal,” <http://hallaweb.jlab.org/parity/prex/> (2005).
- [8] A. Tamii *et al.*, *Phys. Rev. Lett.* **107**, 062502 (2011), arXiv:1104.5431 [nucl-ex].
- [9] J. Birkhan *et al.*, *Phys. Rev. Lett.* **118**, 252501 (2017), arXiv:1611.07072 [nucl-ex].
- [10] R. F. Carlson, A. J. Cox, N. E. Davison, T. Eliyakut-Roshko, R. H. McCamis, and W. T. H. v. Oers, *Phys. Rev. C* **49**, 3090 (1994).
- [11] M. Tanaka *et al.*, *Phys. Rev. Lett.* **124**, 102501 (2020), arXiv:1911.05262 [nucl-ex].
- [12] I. Angeli and K. P. Marinova, *Atom. Data Nucl. Data Tabl.* **99**, 69 (2013).
- [13] G. Hagen, T. Papenbrock, M. Hjorth-Jensen, and D. J. Dean, *Rept. Prog. Phys.* **77**, 096302 (2014), arXiv:1312.7872 [nucl-th].
- [14] G. Hagen *et al.*, *Nature Phys.* **12**, 186 (2015), arXiv:1509.07169 [nucl-th].
- [15] M. Kohno, *Phys. Rev. C* **86**, 061301 (2012), arXiv:1209.5048 [nucl-th].
- [16] M. Toyokawa, M. Yahiro, T. Matsumoto, and M. Kohno, *PTEP* **2018**, 023D03 (2018), arXiv:1712.07033 [nucl-th].
- [17] H. V. von Geramb *et al.*, *Phys. Rev. C* **44**, 73 (1991).
- [18] K. Amos and P. J. Dortmans, *Phys. Rev. C* **49**, 1309 (1994).
- [19] S. Tagami, M. Tanaka, M. Takechi, M. Fukuda, and M. Yahiro, *Phys. Rev. C* **101**, 014620 (2020), arXiv:1911.05417 [nucl-th].
- [20] M. Toyokawa, K. Minomo, M. Kohno, and M. Yahiro, *J. Phys. G* **42**, 025104 (2015), [Erratum: *J. Phys. G* **44**, 079502 (2017)], arXiv:1404.6895 [nucl-th].
- [21] M. Toyokawa, M. Yahiro, T. Matsumoto, K. Minomo, K. Ogata, and M. Kohno, *Phys. Rev. C* **92**, 024618 (2015), [Erratum: *Phys. Rev. C* **96**, 059905 (2017)], arXiv:1507.02807 [nucl-th].
- [22] M. Takechi *et al.*, *Phys. Rev. C* **79**, 061601 (2009).
- [23] T. Sumi, K. Minomo, S. Tagami, M. Kimura, T. Matsumoto, K. Ogata, Y. R. Shimizu, and M. Yahiro, *Phys. Rev. C* **85**, 064613 (2012), arXiv:1201.2497 [nucl-th].
- [24] E. Chabanat, P. Bonche, P. Haensel, J. Meyer, and R. Schaeffer, *Nucl. Phys. A* **635**, 231 (1998), [Erratum: *Nucl. Phys. A* **643**, 441–441 (1998)].
- [25] E. Chabanat, J. Meyer, P. Bonche, R. Schaeffer, and P. Haensel, *Nucl. Phys. A* **627**, 710 (1997).
- [26] N. Schunck *et al.*, *Comput. Phys. Commun.* **216**, 145 (2017), arXiv:1612.05314 [nucl-th].
- [27] K. Minomo, K. Ogata, M. Kohno, Y. R. Shimizu, and M. Yahiro, *J. Phys. G* **37**, 085011 (2010), arXiv:0911.1184 [nucl-th].
- [28] S. Watanabe *et al.*, *Phys. Rev. C* **89**, 044610 (2014), arXiv:1404.2373 [nucl-th].
- [29] F. A. Brieva and J. R. Rook, *Nucl. Phys.* **291**, 299 (1977).
- [30] F. A. Brieva and J. R. Rook, *Nucl. Phys.* **291**, 317 (1977).
- [31] F. A. Brieva and J. R. Rook, *Nucl. Phys.* **297**, 206 (1978).
- [32] H. de Vries, C. W. de Jager, and C. de Vries, *At. Data Nucl. Data Tables* **36**, 495 (1987).
- [33] S. Goriely, S. Hilaire, M. Girod, and S. Peru, *Phys. Rev. Lett.* **102**, 242501 (2009).
- [34] L. M. Robledo, T. R. Rodríguez, and R. R. Rodríguez-Guzmán, *J. Phys. G* **46**, 013001 (2019), arXiv:1807.02518 [nucl-th].
- [35] I. Angeli and K. Marinova, *At. Data Nucl. Data Tables* **99**, 69 (2013).
- [36] S. Tagami, N. Yasutake, M. Fukuda, and M. Yahiro, (2020), arXiv:2003.06168 [nucl-th].